Electronic Supplementary Material (ESI) for Inorganic Chemistry Frontiers.

Supplementary Information

Coordination Catalysis of Metal and Polydopamine Enables Controlled Release of CO from MnCO by Enhancing Oxidative Stress and Thermal Effect

Wen-Xin Zhang, Lin-Yu Li, Yang Shu, Jian-Hua Wang* *

Department of Chemistry, College of Sciences, Northeastern University, Box 332, Shenyang 110819, China

*Corresponding author

E-mail address: shuyang@mail.neu.edu.cn (Y. Shu), jianhuajrz@mail.neu.edu.cn (J.H. Wang).

Materials

Manganese carbonyl ($Mn_2(CO)_{10}$, abbreviated as MnCO), dopamine (DA), Zinc nitrate hexahydrate ($Zn(NO_3)_2•6H_2O$), 2-Methylimidazole (2-MIM), hemoglobin (Hb), and sodium dithionite (SDT) were obtained from Macklin Biochemical Technology Co., Ltd. 30% hydrogen peroxide (H_2O_2), Methylene blue (MB), L-Glutathione reduced (GSH) and 5,5'-dithio bis-(2-nitrobenzoic acid) (DTNB) were received from Aladdin Reagent Co., Ltd. Phosphate buffered solution (PBS) and roswell park memorial institute (RPMI) 1640 cell culture medium were achieved from Procell Life Science&Technology Co., Ltd. Fetal bovine serum (FBS) was obtained from TransGen Biotechnology Co., Ltd. The calcein-AM/PI live/dead cell staining kit was acquired from Beijing Solarbio Science & Technology Co., Ltd. 5,5′,6,6′-tetrachloro-1,1′,3,3′-tetraethylimidacarbocyanine (JC-1) was obtained from MCE Biotechnology Co., Ltd. 4′,6-Diamidino-2-phenylindole (DAPI) and 2′,7′-dichlorofluoresceindiacetate (DCFH-DA) were purchased from Beyotime biotech. Co., Ltd. Calregulin polyclonal antibody, HMG-1 polyclonal antibody, and goat anti rabbit IgG (H&L)-Alexa Fluor 635 were provided by from ImmunoWay Biotechnology Co., Ltd. The aqueous solution used in the experiment was prepared from deionized water from Milli-Q water purification system.

Instrumentation

The morphology of the prepared nanoparticles was examined using transmission electron microscopy (TEM, JEM-1400PLUS, Japan). Dynamic light scattering (DLS, Malvern Zetasizer Nano ZS, UK) was used to acquire the size distribution and zeta potential of the nanoparticles. The absorption spectra were recorded by adopting UV–vis spectrophotometer (U-3900, USA). A confocal laser scanning microscope (CLSM, FV1200, Japan) was used to obtain cellular images. Optical density (OD) was recorded by using Synergy H1 Hybrid Technology (Biotek, USA). The contents of Mn were detected by inductively coupled plasma mass spectrometry (ICP-MS, 8900, USA).

Preparation of MnCO@ZIF (ZM) and MnCO@ZIF@PDA (ZMP)

MnCO@ZIF (denoted as ZM) was prepared using one-pot encapsulation[1]. In short, 2-Mein (0.68 g) was dissolved in 20 mL of methanol, followed by drop-wisely addition of 2 mL MnCO and $Zn(NO_3)_2$•$6H_2O$ mixture solution, and the solution was stirred for 1 h. The product was afterwards collected by centrifugation for 5 min at 8000 rpm and washed three times with methanol. ZM nanoparticles were obtained at 50 ℃ by vacuum drying. ZIF-8 nanoparticles were obtained similarly, in which MnCO was not involved in the mixed solution.

5 mL of ZM solution (5 mg/mL) was mixed with 15 mL of Tris-HCl solution (pH 8.5). 20 mg of DA was then added into the above mixture and kept stirring for 0.5 h to produce ZIF-8/MnCO@PDA (denoted as ZMP) nanoparticles. The product was collected by centrifugation at 8000 rpm for 5 min, followed by washing three times with deionized water, and finally freeze-dried for 24 h.

Photothermal capability of ZMP NPs

Different concentrations of ZMP NPs (50, 100, 200, 300 $mg \cdot L^{-1}$) were irradiated in a quartz cuvette by an NIR laser at various power densities (0.8, 1.0 and 1.5 $W \cdot cm^{-2}$) for 10 min and the temperature changes were recorded. The thermal images were also recorded using an infrared thermal imaging camera (Fluke Ti400).

***In vitro* CO release**

CO release was measured by a standard hemoglobin (Hb) assay[2, 3]. Briefly, bovine Hb was dissolved in PBS at pH 7.4. The Hb solution (2 mg mL^{-1}, 1 mL) was then reduced by sodium dithionite (SDT, 0.1 M, 1 mL) for 10 min. Afterwards, 200 μL ZMP dispersion (200 μg mL^{-1}) and H_2O_2 solution (10 μL, 100 mM) were added into 1 mL Hb solution. During the incubation for 60 min, the absorption spectra were measured in the range of 350-500 nm.

CV measurements

A three-electrode cell was used for electrochemical tests with an Ag/AgCl electrode as the reference electrode, a carbon cloth electrode as the working electrode and a carbon rod electrode as the auxiliary electrode. Mild acidic K_2SO_4 buffer solution (pH 6.8) containing Mn^{2+} (0.1 mM) or a mixture of Mn^{2+} (0.1 mM) and DA (0.05 mM) was used for CV measurement (−1.80 and +1.80 V at a scan rate of 10 mV/s).

***In vitro* cellular toxicity test**

4T1 cells were seeded into 96-well plates with a density of 1×10^4 cells/well for 24 h. Then, the cells were treated by ZM group (5, 10, 20 μg mL^{-1}), ZMP group (7.5, 15, 30 μg mL^{-1}) and ZMP + Laser (7.5, 15, 30 μg mL^{-1}; 10 min, 808 nm, 1.0 W cm^{-2}) and cultured for 24 h. Then, the cell viability was determined with the MTT assay.

Intracellular reactive oxygen species (ROS)

4T1 cells were initially plated in 6-well plates at a density of 2×10^5 cells/well and cultured at 37°C for 24 h. Then, the cells were treated by (1) PBS group; (2) ZM group (10 μg mL^{-1}, Zn content: 0.1 μg mL^{-1}); (3) ZMP group (15 μg mL^{-1}, Zn content: 0.1 μg mL^{-1}); (4) ZMP + Laser group (15 μg mL^{-1}, Zn content: 0.1 μg mL^{-1}, 0.1 W cm^{-2}). for 24h. Afterwards, 1 mL of DCFH-DA (10 μM) was added to each well for 25 min at 37 °C. 4T1 cells were subsequently washed with PBS to eliminate any excessive DCFH-DA, and the cells were finally collected to perform flow cytometry analysis.

Changes in mitochondrial membrane potential

4T1 cells were initially plated in 6-well plates and grown for 24 h at 37 °C. Then, the cells were treated by (1) PBS group; (2) ZM group (10 μg mL^{-1}, Zn content: 0.1 μg mL^{-1}); (3) ZMP group (15 μg mL^{-1}, Zn content: 0.1 μg mL^{-1}); (4) ZMP + Laser group (15 μg mL^{-1}, Zn content: 0.1 μg mL^{-1}, 0.1 W cm^{-2}). After 12 h, 1 mL of JC-1

(20 μM) was added to each well and incubated for 20 min at 37 °C. 4T1 cells were subsequently washed with PBS and collected to perform flow cytometry analysis.

Imaging of CO in living cells

CO probe (FL-CO-1) was used to detect intracellularly released CO[4, 5]. 4T1 cells were initially plated in 6-well plates at a density of 2×10^5 cells/well and cultured at 37°C for 24 h. Then, the cells were treated by (1) PBS group; (2) ZM group (10 μg mL^{-1}, Zn content: 0.1 μg mL^{-1}); (3) ZMP group (15 μg mL^{-1}, Zn content: 0.1 μg mL^{-1}); (4) ZMP + Laser group (15 μg mL^{-1}, Zn content: 0.1 μg mL^{-1}, 0.1 W cm^{-2}) for 24h. Afterwards, 1 mL of FL-CO-1 (1 μM) and $PdCl_2$ (1 μM) was added to each well and incubated for 30 min at 37 °C. 4T1 cells were subsequently washed with PBS and were observed using the confocal laser scanning microscope (CLSM).

Evaluation of CRT inversion and HMGB1 release

For immunofluorescence detection of CRT evagination inside the cell membrane, 4T1 cells were seeded into confocal plates and treated with equal volumes of PBS, ZM NPs (10 mg mL^{-1}, Zn content: 0.1 μg mL^{-1}), ZMP NPs (15 mg mL^{-1}, Zn content: 0.1 μg mL^{-1}) or ZMP NPs + laser (15 mg mL^{-1}, Zn content: 0.1 μg mL^{-1}, 0.1 W cm^{-2}), respectively. After 12 h, the cells were washed with PBS for three times and fixed with 4% paraformaldehyde for 10 min. Then, the cells were sealed with 3% BSA for 1 h to remove the interference of non-specific binding and incubated with anti-mouse CRT antibodies for 12 h at 4°C. Thereafter, the cells were further incubated with Alexa Flour 635-conjugated secondary antibody for 1 h at room temperature and staining using DAPI for 20 min. Finally, the cells were washed with PBS and were observed using CLSM.

The immunofluorescence assay for HMGB1 was similar with those described above. Except for that 4T1 cells were permeabilized with 0.3% Triton for 30 min and incubated with anti-mouse HMGB1 antibodies.

In vivo biodistribution of ZMP NPs

All the animal experimental procedures were conducted in compliance with the Northeastern University Guidelines for Care and Use of Laboratory Animals and with the approval of the Northeastern University Animal Ethics Committee (NEU-EC-2022A006S).

To investigate the bio-distribution of ZMP NPs in mice after i.v. injection, the Mn content in the main organs, e.g., heart, liver, spleen, lung and kidney, as well as the tumors were detected. Briefly, 4T1 tumor-bearing mice were i.v. injected with 100 μL ZMP NPs (1.5 mg/ml). After 3, 6, 12 and 24 h, the above mentioned main organs and the tumors were obtained and digested with HNO_3 and H_2O_2. Finally, the content of Mn in the organ tissue and the tumor was detected by ICP-MS.

In vivo antitumor treatments

Female Balb/c mice (6 weeks old, 18∼20 g) were housed under standard settings for 1 week. Then, 100 μL mixture containing 4T1 cells with the amount of 1×10^6 were injected subcutaneously into the rear of each mouse. When the tumor volume reached ∼ 100 mm^3, the mice were randomly divided into four groups (8 mice in each group): (1) PBS group; (2) ZM group (1.0 mg mL^{-1}, Zn content: 0.1 mg mL^{-1}); (3) ZMP group (1.5 mg mL^{-1}, Zn content: 0.1 mg mL^{-1}); (4) ZMP + Laser group (1.5 mg mL^{-1}, Zn content: 0.1 mg mL^{-1}, 0.1 W cm^{-2}). Each mouse was i.v. injected with 100 μL materials for 5 times. Every two days, tumor sizes and weights were measured. After treatment for 14 days, mice blood, the tumors and the main organs were collected and examined.

Statistical analysis

All the experimental data were exhibited as the mean ± standard deviation (SD). The one-way ANOVA was used for the analysis of statistical differences between various groups. Values with $p < 0.05$ were considered statistically significant ($p < 0.05$, $p < 0.01$ and $p < 0.001$ are marked with *, **, and ***, respectively).

Reference

(1) X. Zhang, J.Y. Chen, X. Pei, Y.H. Li, H. Feng, Z.H. He, W.J. Xie, X.B. Pei, Z. Zhu, Q.B. Wan, J. Wang, One-Pot Facile Encapsulation of Dimethyloxallyl Glycine by Nanoscale Zeolitic Imidazolate Frameworks-8 for Enhancing Vascularized Bone Regeneration, Advanced Healthcare Materials 12 (2022), 2202317. https://doi.org/10.1002/adhm.202202317.

(2) G. Yang, T. Song, H. Zhang, M. Li, X. Wei, W. Zhou, C. Wu, Y. Liu, H. Yang, Stimulus-Detonated Biomimetic "Nanobomb" with Controlled Release of HSP90 Inhibitor to Disrupt Mitochondrial Function for Synergistic Gas and Photothermal Therapy, Advanced Healthcare Materials 12 (2023), 2300945. https://doi.org/10.1002/adhm.202300945.

(3) J. Zhang, D. Tong, H. Song, R. Ruan, Y. Sun, Y. Lin, J. Wang, L. Hou, J. Dai, J. Ding, H. Yang, Osteoimmunity-Regulating Biomimetically Hierarchical Scaffold for Augmented Bone Regeneration, Advanced Materials 34 (2022), 2202044. https://doi.org/10.1002/adma.202202044.

(4) D. Zhu, Z. Liu, Y. Li, Q. Huang, L. Xia, K. Li, Delivery of manganese carbonyl to the tumor microenvironment using Tumor-Derived exosomes for cancer gas therapy and low dose radiotherapy, Biomaterials 274 (2021), 120894. https://doi.org/10.1016/j.biomaterials.2021.120894.

(5) Y. Zhou, R. Zhang, Y. Lu, X. Fu, K. Lv, J. Gong, D. Wang, J. Feng, H. Zhang, Y. Guo, Acid-Unlocked Switch Controlled the Enzyme and CO In Situ Release to Induce Mitochondrial Damage via Synergy, Advanced Functional Materials (2024), 2312416. https://doi.org/10.1002/adfm.202312416.

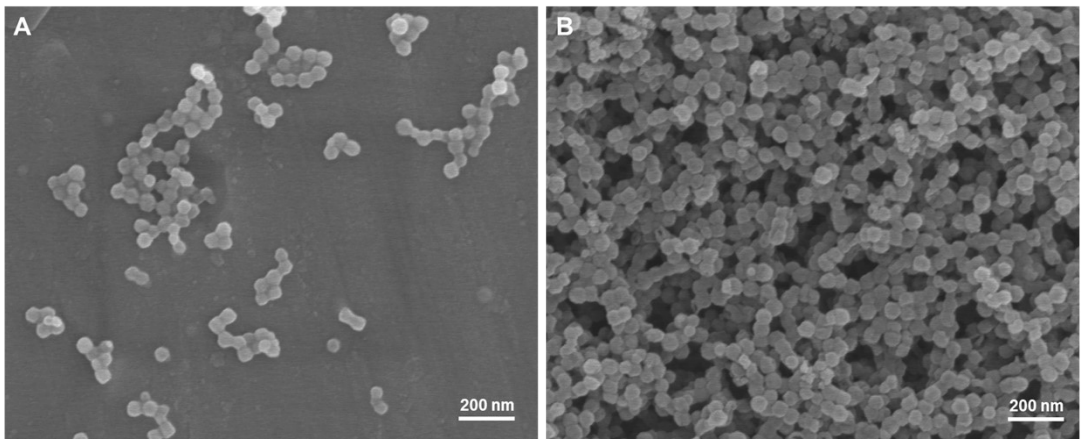

Figure S1. SEM images of (A) ZM NPs and (B) ZMP NPs, with a scale bar of 200 nm.

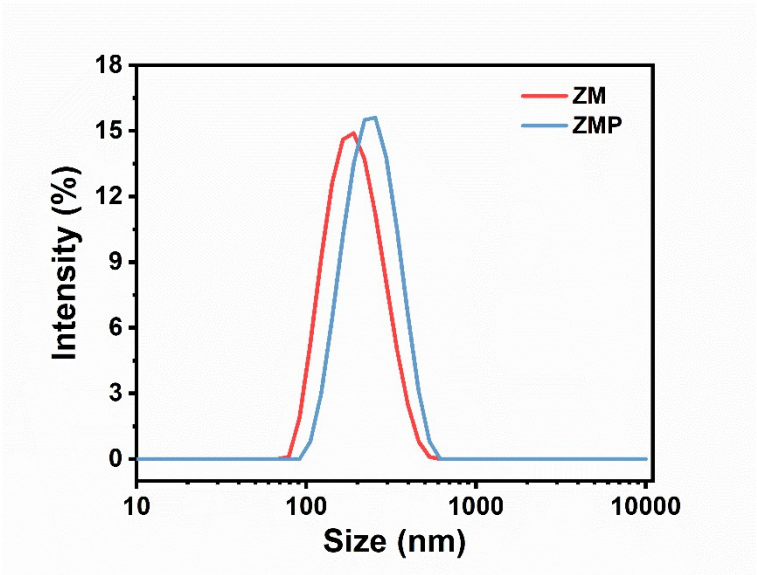

Figure S2. The mean hydrodynamic size distribution of ZM NPs (200 μg mL^{-1}) and ZMP NPs (200 μg mL^{-1}).

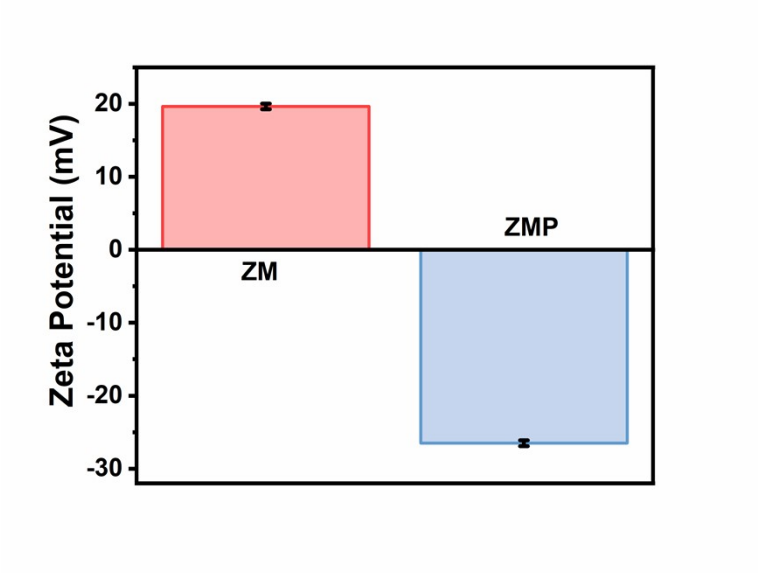

Figure S3. Zeta potential analysis of ZM NPs and ZMP NPs. The data were defined as mean ±S.D. (n=3).

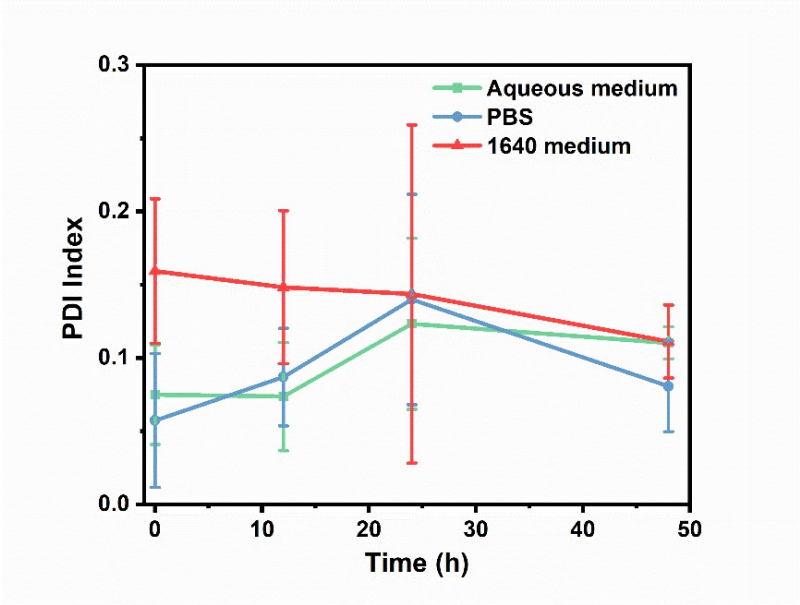

Figure S4. The PDI index of ZMP NPs solutions (200 μg mL^{-1}) in aqueous medium, PBS and RPMI l640 medium within 48 h.

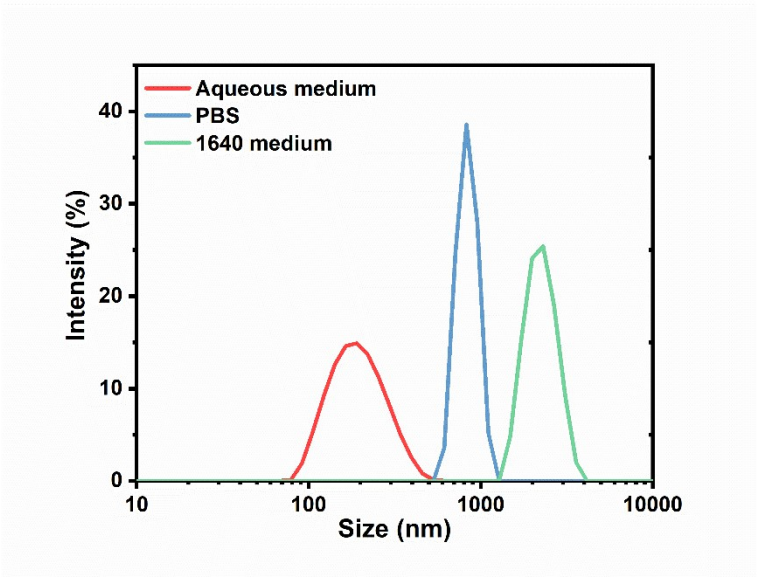

Figure S5. The hydrodynamic diameter of ZM NPs (200 μg mL^{-1}) in aqueous medium, PBS, and RPMI 1640 medium at 24h.

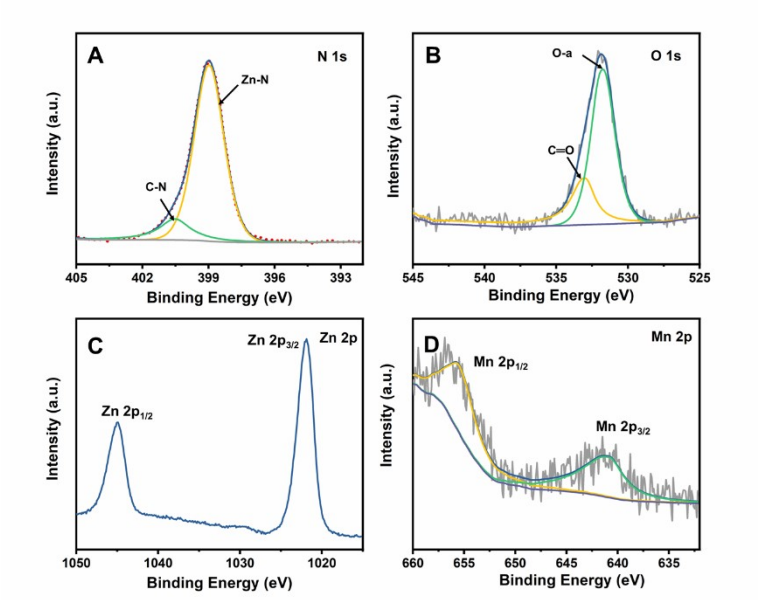

Figure S6. High-resolution (A) N 1s, (B) O 1s, (C) Zn 2p, and Mn 2p XPS spectra of ZM NPs.

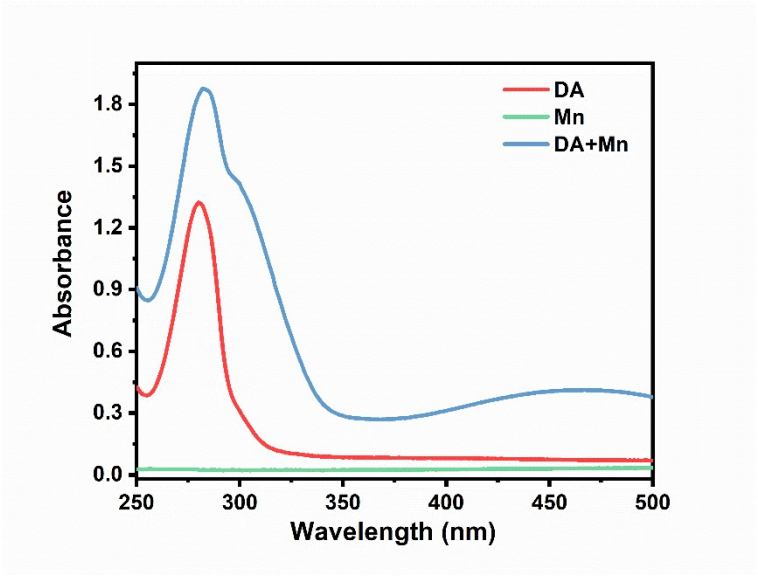

Figure S7. UV–vis absorption spectra of DA (1 mM), Mn^{2+} (1 mM), and DA-Mn (1 mM).

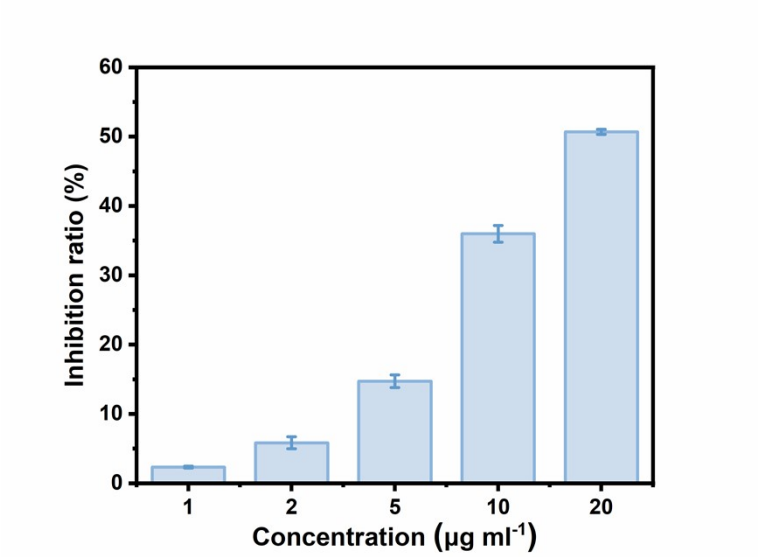

Figure S8. The inhibition effect of ZMP NPs (0-20 μg mL^{-1}) against the production of WST formazan in 20 min.

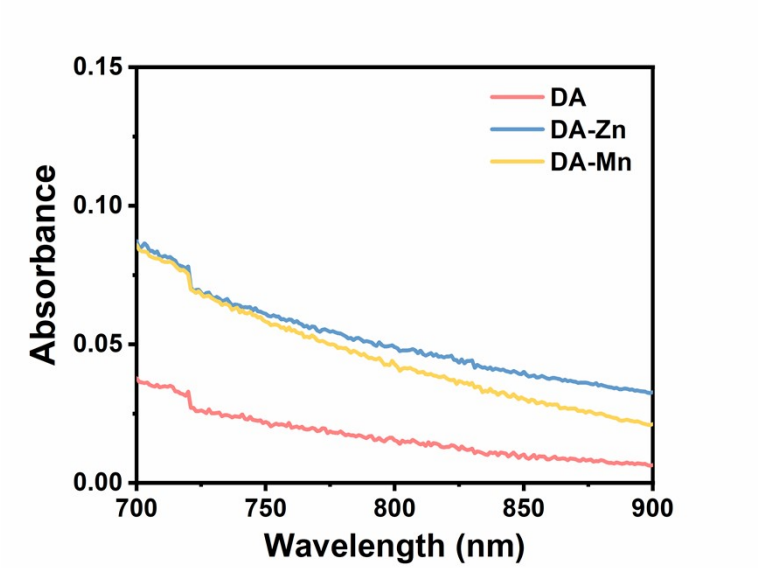

Figure S9. The absorption spectra of DA (50 mM), DA-Zn (50 mM), and DA-Mn (50 mM) solution within the wavelength range of 700-900 nm.

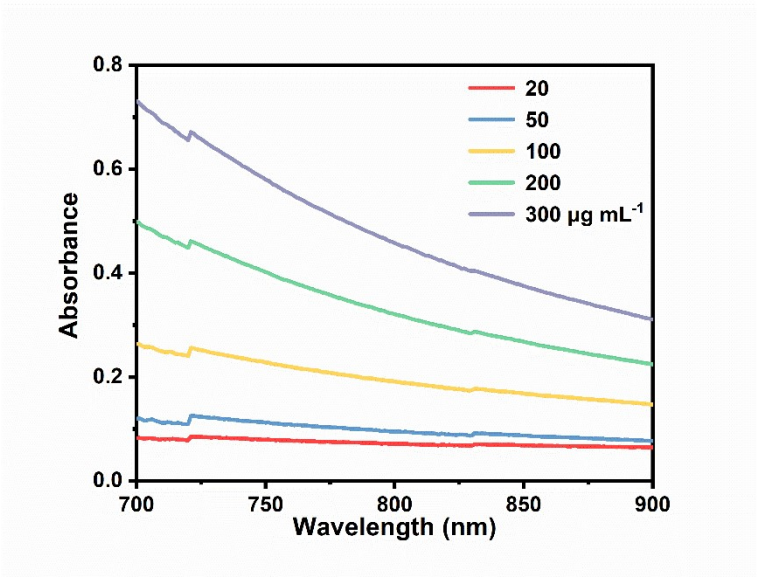

Figure S10. The absorption spectra of ZMP NPs solution with different concentrations (0-300 μg mL^{-1}) within the range of 700-900 nm.

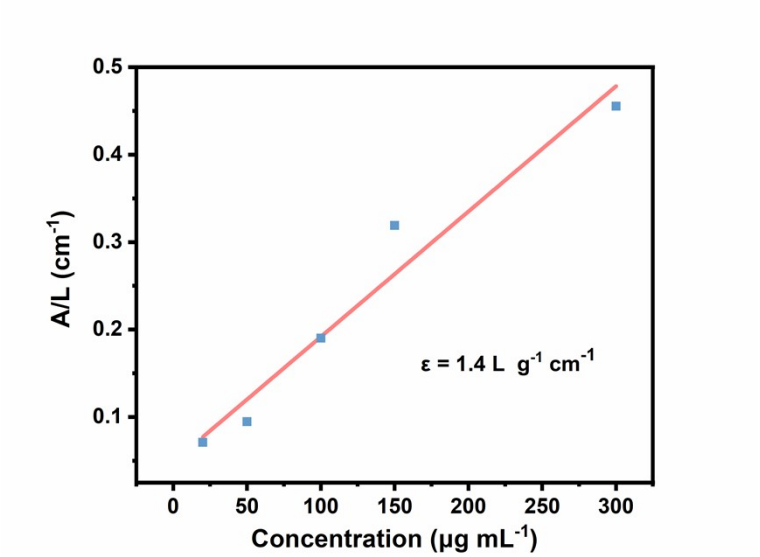

Figure S11. Mass extinction coefficients of ZMP NPs with different concentrations (20, 50, 100, 200, 300 μg mL^{-1}) at 808 nm.

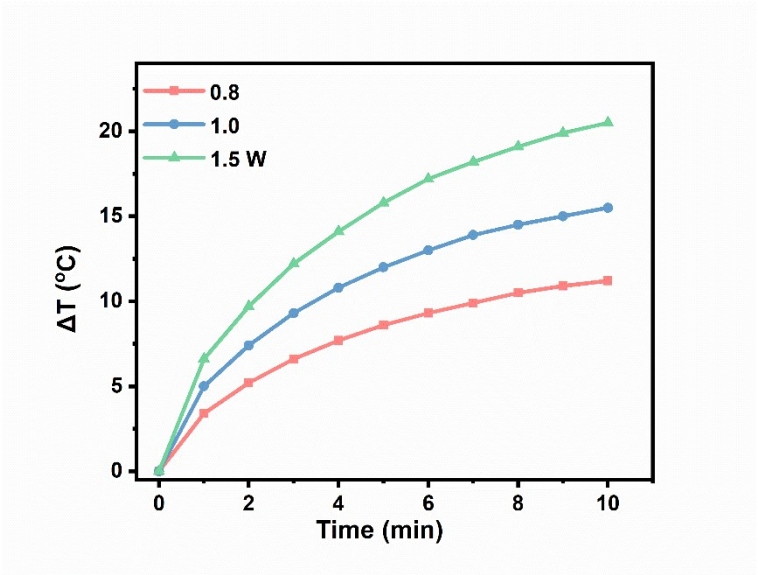

Figure S12. The temperature changes of ZMPs solutions under 808 nm laser irradiation for 10 min withat different power densities (0.8, 1.0, 1.5 W cm^{-2}, 10 min).

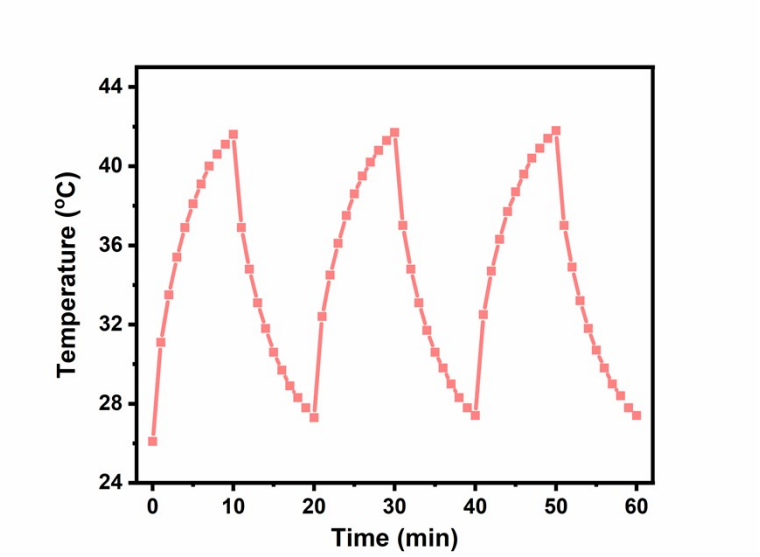

Figure S13. Photothermal stability curve of ZMPs NPs solutions (200 μg mL^{-1}) by three cycles on/off of 808 nm laser irradiation (1.0 W cm^{-2}).

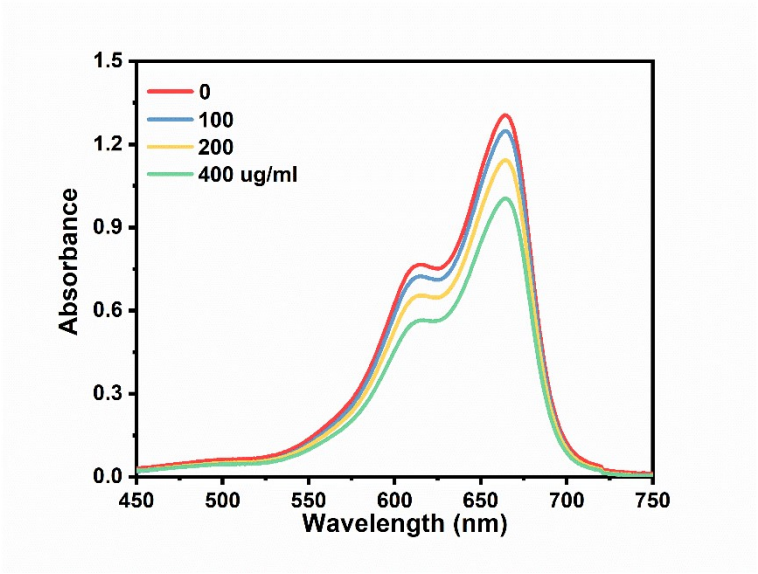

Figure S14. UV–vis absorption spectra of MB degradation under different concentrations (0, 100, 200, 400 μg mL^{-1}) for 2h

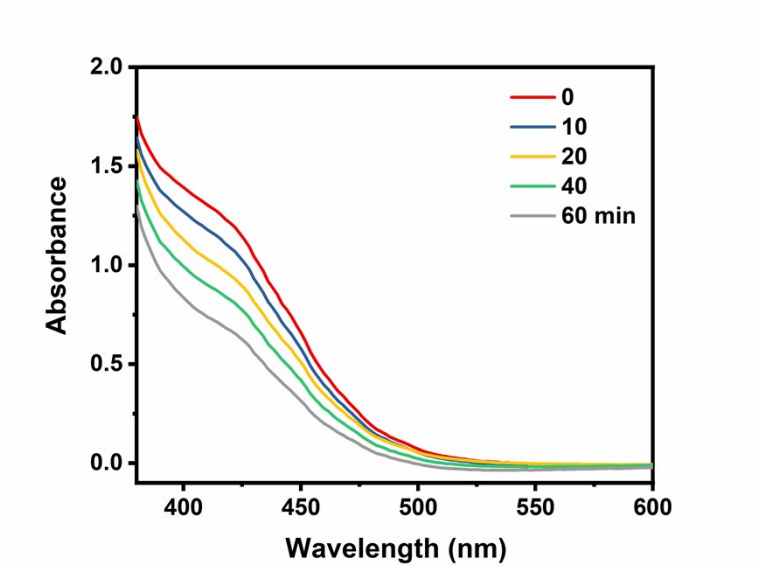

Figure S15. GSH consumption capability of ZMP NPs (50 μg mL^{-1}) within 60 min.

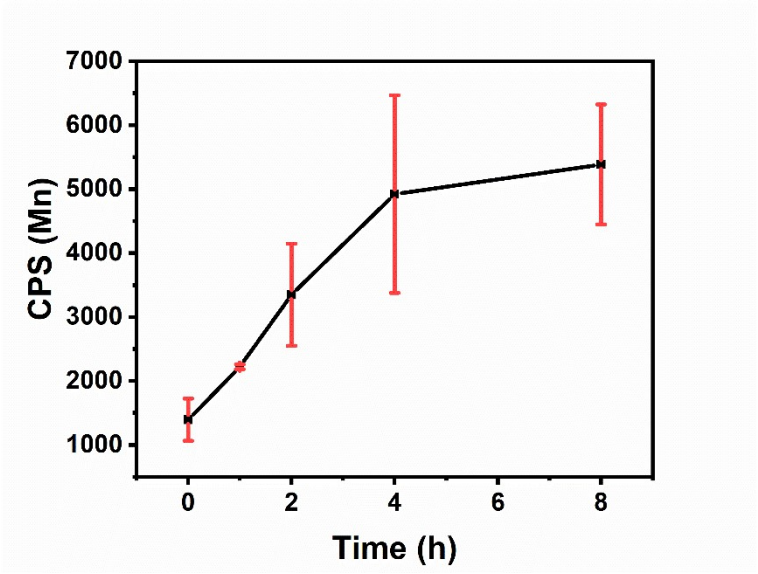

Figure S16. The cellular uptake behavior of ZMP nanoparticles is investigated by ICP-MS at 0, 1, 2, 4, 8h.

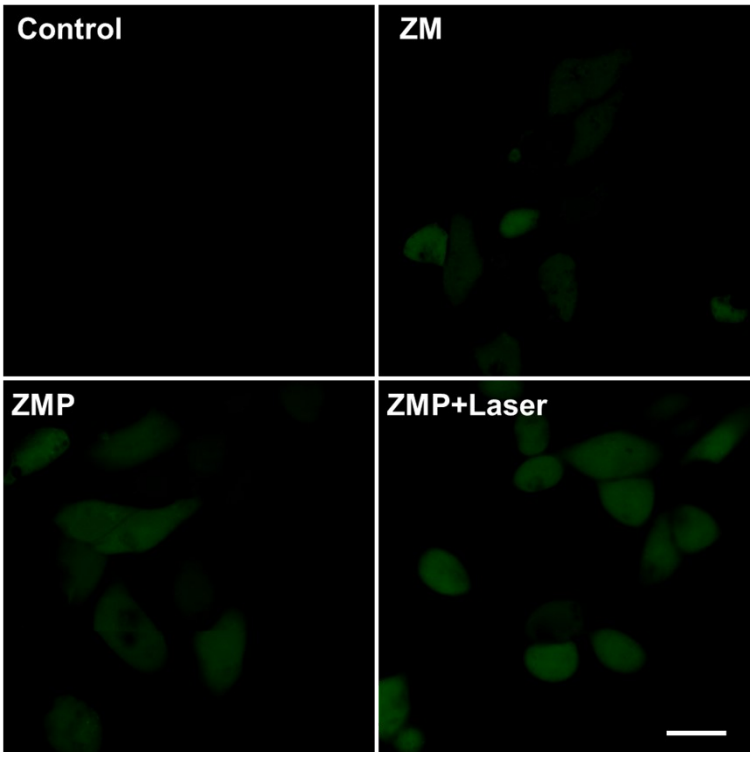

Figure S17. The production of CO in 4T1 cells after treatments by ZM NPs, ZMP NPs, or ZMP NPs + laser irradiation. Scale bar: 20 μm.

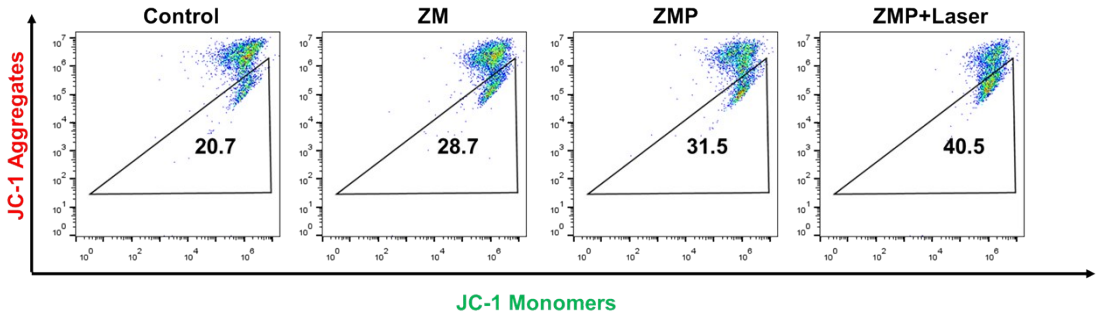

Figure S18. The changes in mitochondrial membrane potential of 4T1 cells after different treatments by using flow cytometry.

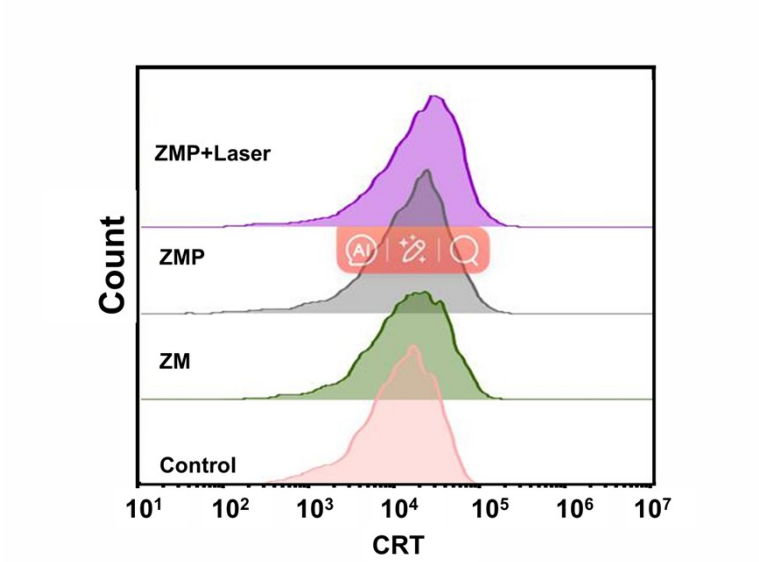

Figure S19. Fluorescent of CRT in 4T1 cells after treatments by ZM NPs, ZMP NPs, or ZMP NPs + laser irradiation with quantitative analysis using flow cytometry.

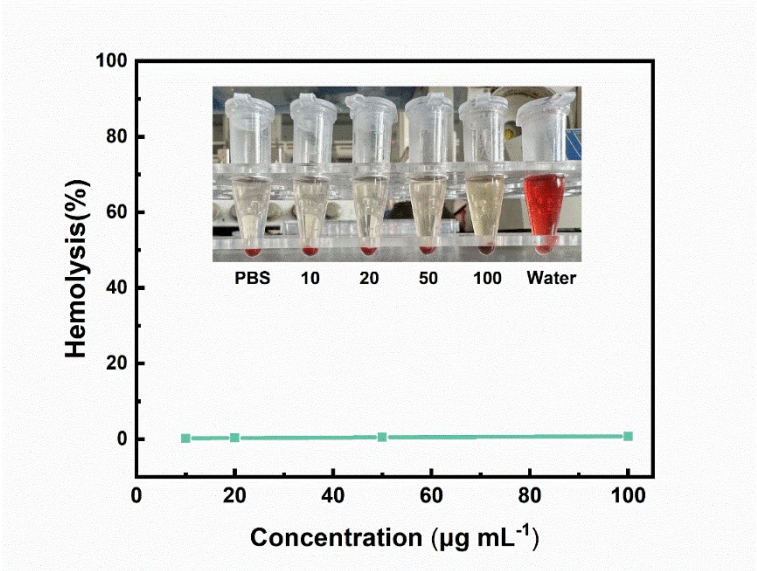

Figure S20. Hemolysis analysis of ZMP NPs at different concentrations (10, 20, 50, 100 μg mL^{-1}). PBS was used as negative control, and deionized water was used as positive control. Inset: the photographs of the above hemolysis assay mixtures (n=3).

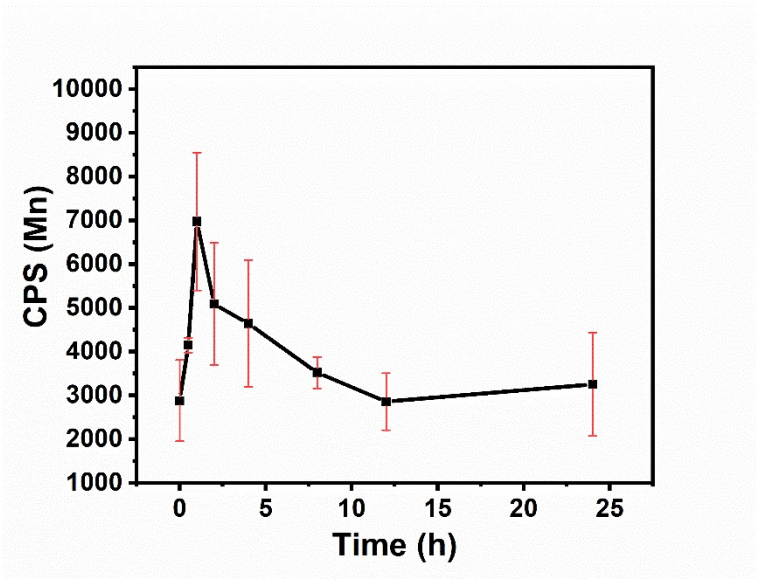

Figure S21. The pharmacokinetics of ZMP in the body at various time point (30 min, 1 h, 2 h, 4 h, 8 h, 12 h, 24 h and 48 h) detected by ICP-MS.

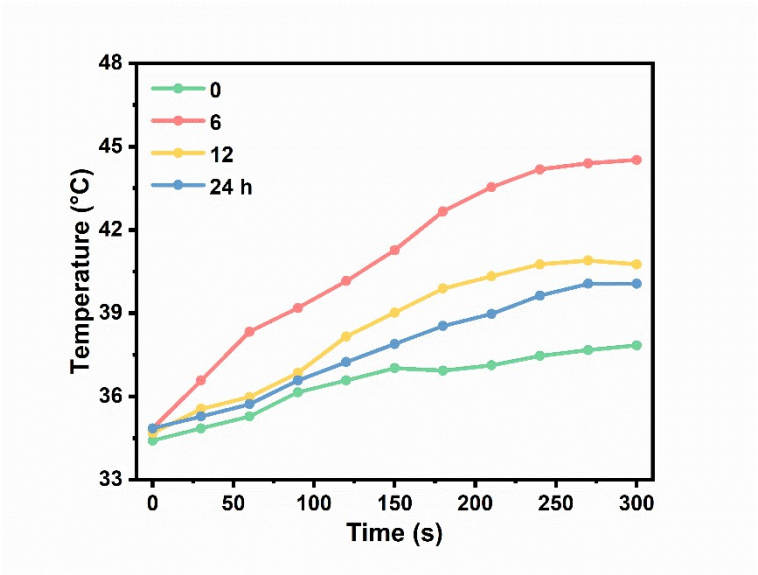

Figure S22. Temperature curves of mice after injection of ZMP NPs for 0, 6, 12, 24 h under 808 nm laser irradiation (5 min, 0.1 W cm^{-2}).

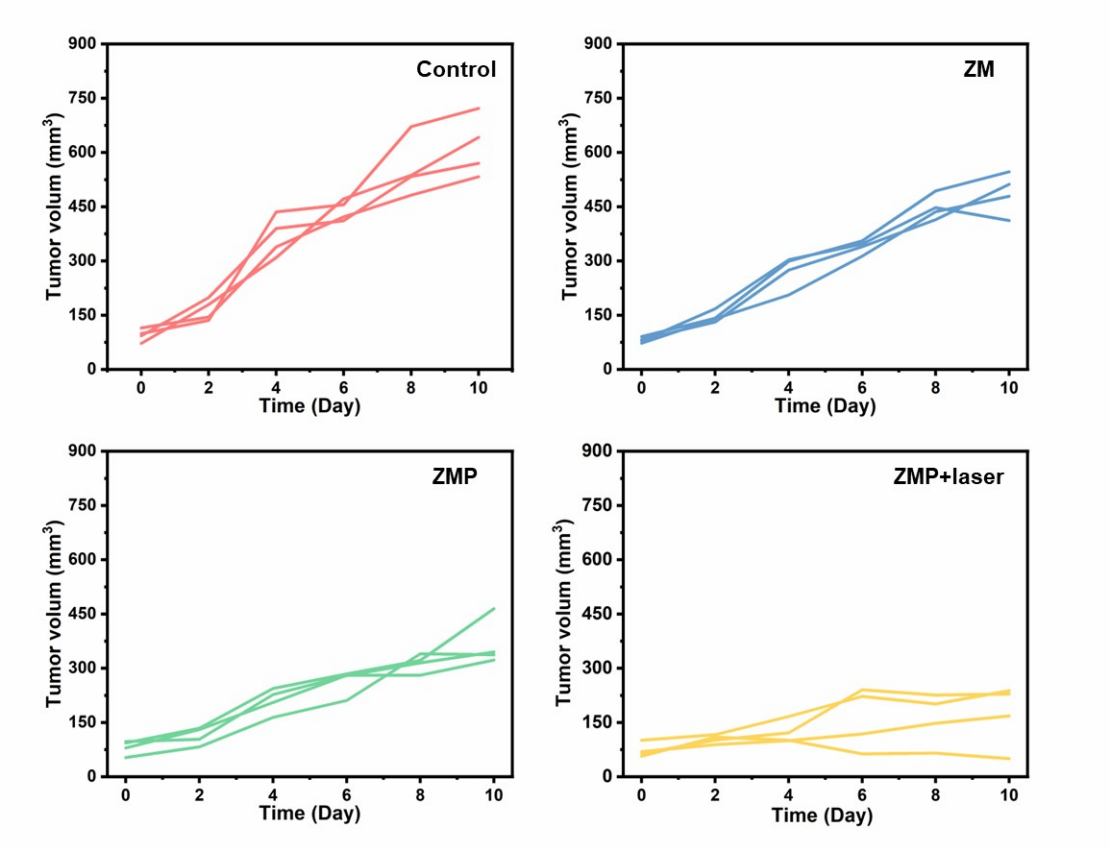

Figure S23. Tumor volume changes of mice in PBS, ZM NPs, ZMP NPs, or ZMP NPs + laser treated groups.

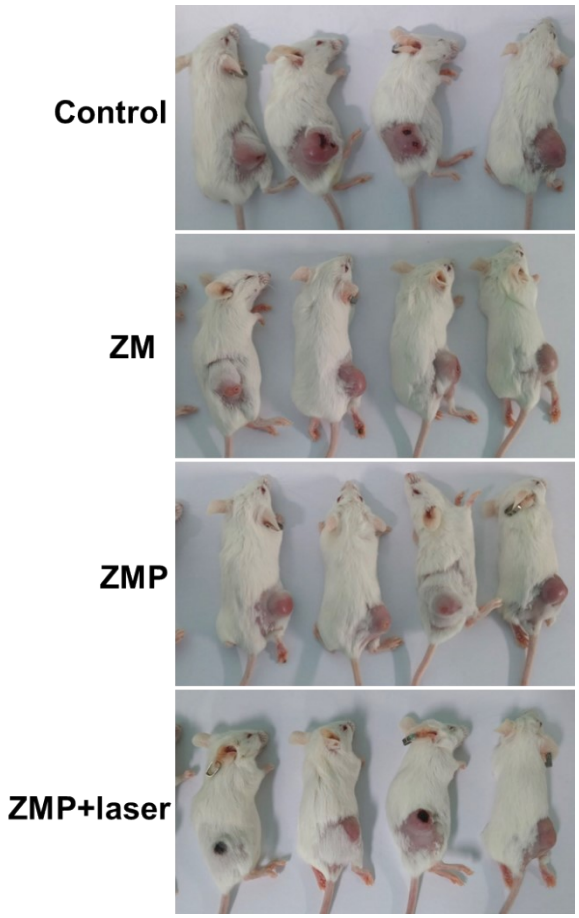

Figure S24. Photographs of mice on day 10 after various treatments.

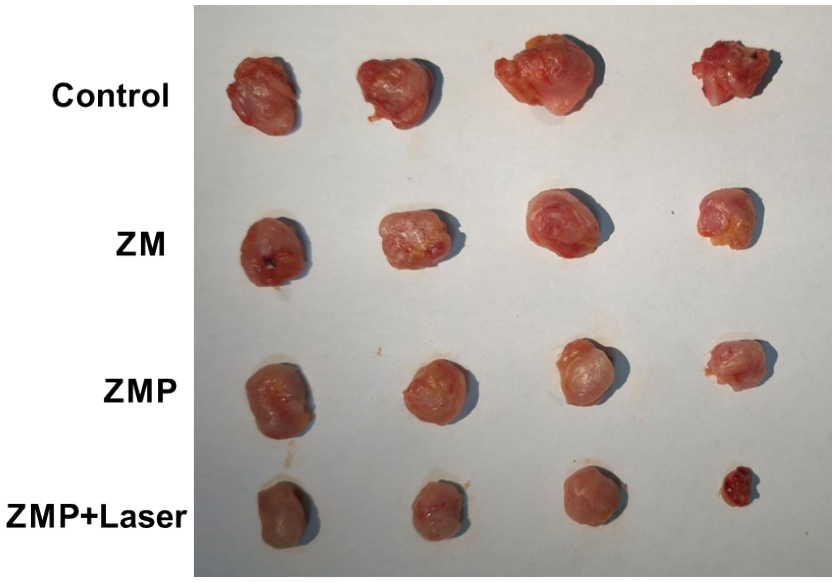

Figure S25. Representative photographs of the dissected tumors on day 10 after various treatments.

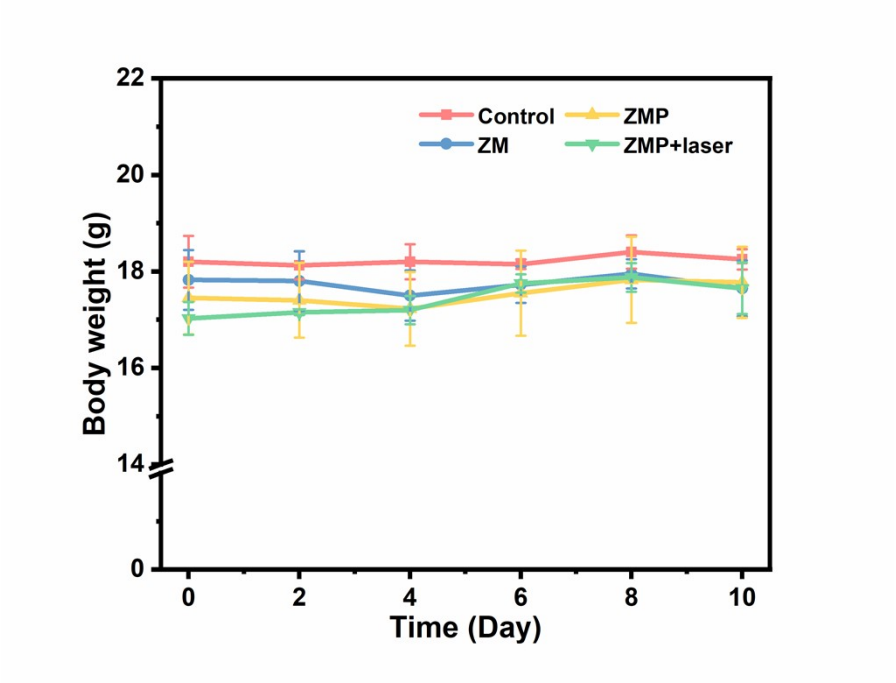

Figure S26.The variations of body weights for the mice bearing 4T1 tumors during the whole period of treatment in the various groups.

Equation S1-S5: The coordination catalysis between Zn and DA